Available online at www.sciencedirect.com
SCIENCE DIRECT®
Journal of Power Sources 115 (2003) 167–170
JOURNAL OF POWER SOURCES
www.elsevier.com/locate/jpowsour

Short communication

Optimization of a combined thermionic–thermoelectric generator

X.C. Xuan, D. Li*

Department of Mechanical and Industrial Engineering, University of Toronto, 5 King's College Road, Toronto, Ont., Canada M5S 3G8

Received 25 October 2002; accepted 13 November 2002

Abstract

A combined thermionic–thermoelectric generator is proposed in this paper. The thermoelectric generator makes use of the rejected heat from the anode of the thermionic generator, and produces additional electrical power. The combined generator system has both improved efficiency and power output. Optimization analysis of the combined generator is presented in this work.

Keywords: Power generator; Thermionic generator; Thermoelectric generator; Combined power system

1. Introduction

Both thermionic [1] and thermoelectric [2] generators employ the electron gas as the working fluid, and convert thermal energy directly into electrical energy without mechanical moving parts [3]. They are simple, reliable and compact. A thermionic generator based on the ballistic current flow is highly efficient, and its theoretical efficiency is close to the Carnot efficiency [4–10]. A thermoelectric generator, however, has poor efficiency due to the diffusive current flow [2,3,10–13]. A thermionic generator usually requires a high-temperature heat source (e.g. 1500 K) to generate a practically useful current [1,3]. A thermoelectric generator, however, can produce electrical power from low-quality heat energy sources [14,15].

In this paper, we show that a thermionic generator can provide approximately the same output in power and efficiency while its anode temperature varies in a significantly large range, as described in Section 2. Therefore, we suggest connecting a thermoelectric generator thermally to the anode of a thermionic generator, so that the heat leaving the anode can be further utilized. Fig. 1 shows the scheme of the combined thermionic–thermoelectric generator. This structure is different from the combined thermionic–thermoelectric refrigerator proposed recently [16]. In the combined refrigerator, the thermionic diode and thermoelectric element are thermally connected in parallel but electrically connected in series. In the combined electrical generator, however, thermionic and thermoelectric devices are electrically separated, and the sole communication between them is the heat exchange. The optimal performance of the combined generator system is discussed in Section 3.

2. Thermionic generator

This section will review the standard theory of a vacuum thermionic generator. The analysis shows that both the output power and the efficiency of a vacuum thermionic generator are insensitive to the anode temperature over a range. In the presence of space-charge effect, the potential diagram of a vacuum thermionic generator is shown in Fig. 2. The subscripts c and a denote the cathode and anode, respectively. ϕ is the work function of electrodes, and V indicates the potential difference between the top of the potential barrier (i.e. the potential minimum) and the Fermi level. It is obvious that $V_{c,a} \geq \phi_{c,a}$. V_{TI} is the potential drop across the external load, where the subscript TI is the abbreviation of thermionic. Note that V_{TI} has included the potential drop in the necessary electrical connection to the electrodes. Hence, we can avoid complicated calculations of the conductive and Joulean heat arising from lead wires. It follows that $V_c = V_a + V_{TI}$.

The net current density J_{TI} (i.e. electrical current per unit area of electrodes. The cathode and anode possess the same emissive area) in the generator is equal to $J_c - J_a$ with J_c and J_a being the current densities from the cathode and anode,

* Corresponding author. Tel.: +1-416-978-1282; fax: +1-416-978-7753.
E-mail address: dli@mie.utoronto.ca (D. Li).

0378-7753/02/$ – see front matter
PII: S0378-7753(02)00620-1

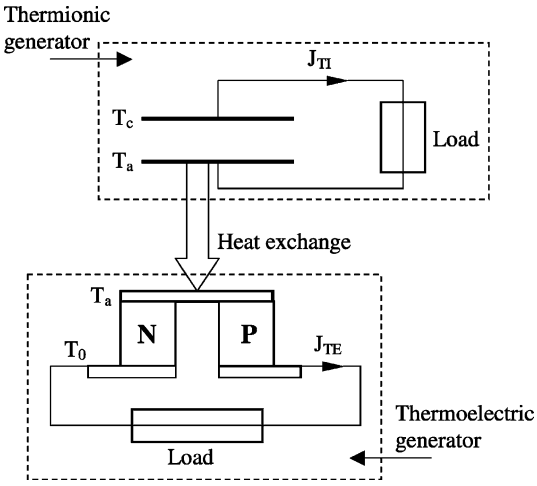

Fig. 1. Scheme of a combined thermionic–thermoelectric generator.

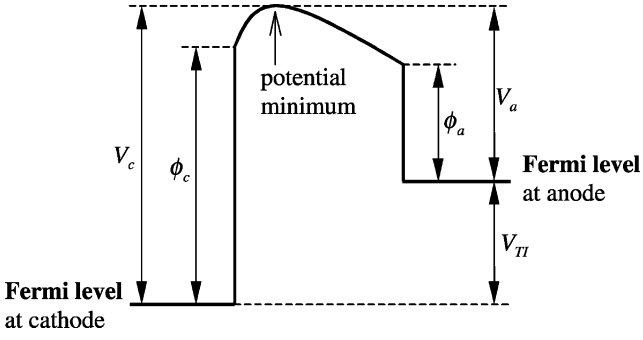

Fig. 2. Potential diagram for a vacuum thermionic generator.

respectively, which are given by Richardson–Dushman equation

$$J_c = AT_c^2 \exp\left(\frac{-eV_c}{\kappa T_c}\right) = AT_c^2 \exp\left(\frac{-eV_a}{\kappa T_c}\right) \exp\left(\frac{-eV_{TI}}{\kappa T_c}\right), \quad (1)$$

$$J_a = AT_a^2 \exp\left(\frac{-eV_a}{\kappa T_a}\right), \quad (2)$$

where T is the absolute temperature of electrodes; $A = 120\ \mathrm{A\ cm^{-2}\ K^{-2}}$, the theoretical thermionic constant; $e = 1.60 \times 10^{-19}$ C, the electron charge and $\kappa = 1.38 \times 10^{-23}\ \mathrm{J\ K^{-1}}$, the Boltzmann constant. The output power density P_{TI} and efficiency η_{TI} defined as the output power density divided by the input heat flow density Q_{in} at the cathode, are then given by

$$P_{TI} = J_{TI} V_{TI}, \quad (3)$$

$$\eta_{TI} = \frac{P_{TI}}{Q_{in}} = \frac{J_{TI} V_{TI}}{J_c(V_a + V_{TI} + 2\kappa T_c) - J_a(V_a + V_{TI} + 2\kappa T_a) + P_r}, \quad (4)$$

$$P_r = \varepsilon\sigma(T_c^4 - T_a^4), \quad (5)$$

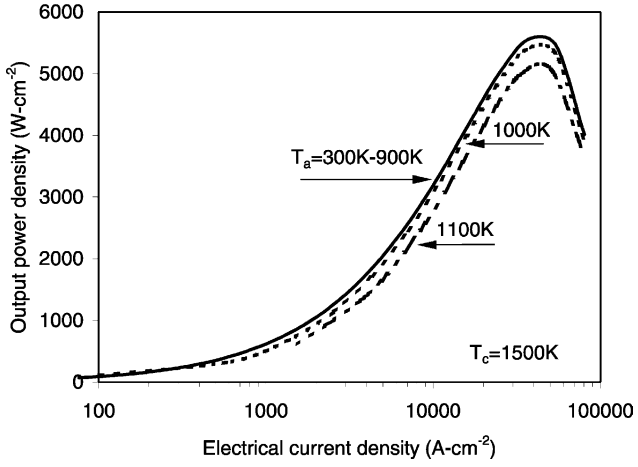

Fig. 3. Output power density against current density for a vacuum thermionic generator.

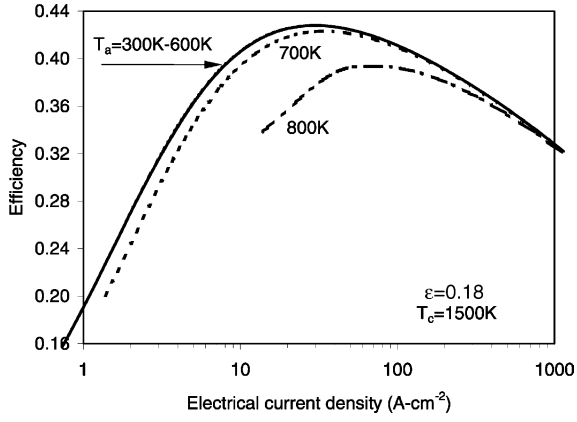

Fig. 4. Efficiency against current density for a vacuum thermionic generator.

where P_r is the radiation heat power density from cathode to anode, ε the effective emissivity[1] of the cathode and $\sigma = 5.67 \times 10^{-8}\ \mathrm{W\ m^{-2}\ K^{-4}}$, the Stefan–Boltzmann constant. It has been assumed that the heat loss through the structural support of cathode can be neglected.

At given operating conditions, P_{TI} and η_{TI} are functions of V_a and V_{TI} or J_{TI}. The magnitude of V_a is dependent on the work function of anode ϕ_a and the space-charge effect as well. It is already known that V_a should be as low as possible in order to obtain the optimum efficiency [4–10]. However, the minimum attainable work function so far is approximately 0.7 V on semiconductor surfaces [17]. Therefore, we choose $V_a = 1$ V as an example throughout this work. The output power density and efficiency against J_{TI} are illustrated in Figs. 3 and 4, respectively, for different anode

[1] For radiation between infinite, plane-parallel electrodes, the effective emissivity is given by $\varepsilon_{eff} = 1/[(1/\varepsilon_c) + (1/\varepsilon_a) - 1]$, where ε_c and ε_a are the emissivities of the cathode and anode, respectively. In this work, we assume $\varepsilon_a = 1$ so that $\varepsilon_{eff} = \varepsilon_c$.

temperature T_a. From these figures, it is clear that there is a sufficiently wide temperature range in which the performance is approximately the same. Therefore, it is possible that, without affecting appreciably the performance of the thermionic generator, we can utilize a relatively large temperature difference between the anode temperature T_a and the room temperature to drive a thermoelectric generator, so that additional electrical power can be produced. This motivates us to propose a combined thermionic–thermoelectric generator, which will be discussed in the next section.

3. Thermionic–thermoelectric generator

In a combined thermionic–thermoelectric generator system, the thermoelectric generator exploits the unused heating power at the anode of the thermionic generator, and has independent return circuit as shown in Fig. 1. It is therefore natural to optimize the thermoelectric generator so that both the overall power output and efficiency of the combined generator system can be maximized.[2] We assume that the p- and n-type thermoelements of the thermoelectric generator are of both structural and characteristic symmetry except the sign of the Seebeck coefficient.

For a thermoelectric generator at average transport coefficients taken at the mean temperature of the device $\bar{T} = (T_a + T_0)/2$, the efficiency η_{TE} is given by

$$\eta_{TE} = \frac{J_{TE}\alpha\,\Delta T - J_{TE}^2\rho L}{J_{TE}\alpha T_a + (k\,\Delta T/L) - (1/2)J_{TE}^2\rho L}, \tag{6}$$

where $\Delta T = T_a - T_0$ with the room temperature T_0, J_{TE} the current density flowing through the thermoelectric generating system (different from J_{TI}, it denotes electrical current per unit area of thermoelements), α, ρ and k the Seebeck coefficient, electrical resistivity and thermal conductivity of thermoelectric materials, respectively, and L the length of thermoelements. The subscript TE is the abbreviation of thermoelectric. The maximum efficiency is found by solving for the value of current density $J_{TE,max}$ which gives the maximum efficiency $\eta_{TE,max}$,

$$J_{TE,max} = \frac{(M-1)(k/L)\,\Delta T}{\alpha\bar{T}}, \tag{7}$$

$$\eta_{TE,max} = \frac{(M-1)\,\Delta T}{MT_a + T_0}, \tag{8}$$

$$M = \sqrt{1 + Z\bar{T}}, \quad Z = \frac{\alpha^2}{\rho k}, \tag{9}$$

where Z is the so-called figure of merit.

As the thermoelectric generator is optimized, the overall output power density P and efficiency η of the combined thermionic–thermoelectric generator system are given by

$$P = P_{TI} + P_{TE}, \tag{10}$$

$$P_{TE} = (Q_{in} - P_{TI})\eta_{TE,max} = Q_{in}(1 - \eta_{TI})\eta_{TE,max}, \tag{11}$$

$$\eta = \frac{P}{Q_{in}} = \eta_{TI} + (1 - \eta_{TI})\eta_{TE,max}, \tag{12}$$

where P_{TE} is the output power density of the thermoelectric generator. P and η are functions of J_{TI} and T_a at a given V_a. At various T_a, we can determine first the corresponding optimum V_{TI} by solving

$$\left(\frac{\partial P}{\partial V_{TI}}\right)_{T_a} = 0 \quad \text{and} \quad \left(\frac{\partial \eta}{\partial V_{TI}}\right)_{T_a} = 0. \tag{13}$$

Then, the maximum P and η of the combined generator can be calculated as well as the optimum J_{TI}. If the length of thermoelements L is given, $J_{TE,max}$ can be calculated from Eq. (7). The cross-sectional area of thermoelements S_{TE} is received from the energy conservation equation at the junction between thermionic and thermoelectric generators. That is

$$S[J_c(V_a + 2\kappa T_c) - J_a(V_a + 2\kappa T_a) + P_r] = 2S_{TE}\left(\frac{k}{L}\right)(T_a - T_0)\left[\frac{M}{M+1}\right]\left[\frac{2 + ZT_a}{M+1}\right], \tag{14}$$

where S is the area of thermionic electrodes.

The properties of commercial Bi_2Te_3-based thermoelectric materials are selected in our calculations. The specific equations for computing these properties are listed in the Appendix A. Figs. 5 and 6 show the performances with respect to T_a in terms of the maximum power output and

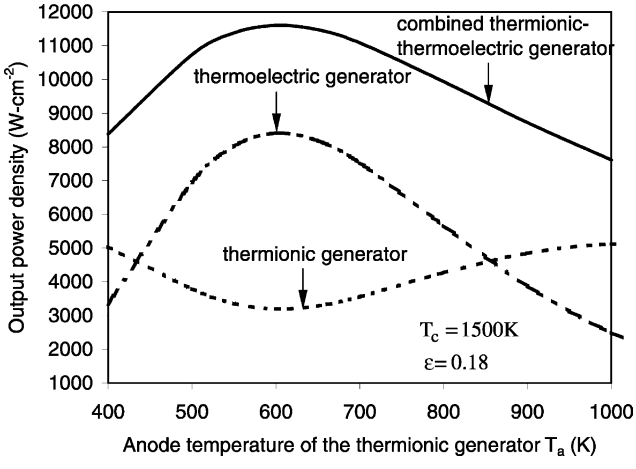

Fig. 5. Output power density of the combined thermionic–thermoelectric generator against the anode temperature T_a of the thermionic generator. The other two curves for the thermionic and thermoelectric devices are calculated from the parameters corresponding to the optimal combined generator.

[2] As described below, the anode temperature T_a is the sole parameter that affects the performance of both thermionic and thermoelectric generators. It is therefore reasonable to optimize the thermoelectric generator first with respect to its operating current given a T_a.

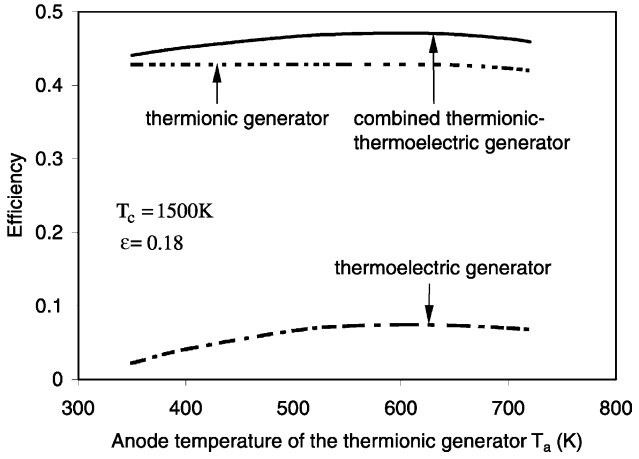

Fig. 6. Efficiency of the combined thermionic–thermoelectric generator against the anode temperature T_a of thermionic generator. The other two curves for the thermionic and thermoelectric devices are calculated from the parameters corresponding to the optimal combined generator.

efficiency, respectively. As expected, there exists an optimum value of T_a at which P or η is maximized. In comparison with the performance of a vacuum thermionic generator as shown in Figs. 3 and 4, the performance improvement of the combined thermionic–thermoelectric generator system is obvious, especially the output power density. Realizing that Bi_2Te_3-based semiconductors are not the best thermoelectric materials over the temperature range of 300–600 K [18,19], one can expect a significant increase in the performance if better materials are employed.

4. Conclusions

We have shown that the combined thermionic–thermoelectric generator system can provide not only more electrical power but also higher efficiency than a vacuum thermionic converter or a thermoelectric generator. Since this combined generator system requires separate thermionic and thermoelectric generating circuits, this may complicate the system and its matching with external loads. Better thermoelectric materials over the temperature range of 300–600 K or higher can further improve the performance of the combined generator system.

Acknowledgements

Financial support from the Natural Sciences and Engineering Research Council (NSERC) of Canada, through a research grant to D. Li is gratefully acknowledged.

Appendix A

Commercial Bi_2Te_3-based thermoelectric materials selected in this work are available from MELCOR, USA. The property formulas with respect to the mean temperature $\bar{T}$ are given by [20]

$$\alpha\,(\mathrm{V\,K^{-1}}) = (22224.0 + 930.6\,\bar{T} - 0.9905\,\bar{T}^2) \times 10^{-9}, \tag{A.1}$$

$$\rho\,(\Omega\,\mathrm{m^{-1}}) = (5112.0 + 163.4\,\bar{T} + 0.6279\,\bar{T}^2) \times 10^{-10}, \tag{A.2}$$

$$k\,(\mathrm{W\,m^{-1}\,K^{-1}}) = (62605.0 - 277.7\,\bar{T} + 0.4131\,\bar{T}^2) \times 10^{-4}. \tag{A.3}$$

References

[1] G.N. Hatsopoulos, E.P. Gyftopoulos, Thermionic Energy Conversion, MIT Press, Cambridge, MA, 1973.
[2] H.J. Goldsmid, Electronic Refrigeration, Pion Limited, London, 1986.
[3] J. Kaye, J.A. Welsh, Direct Conversion of Heat to Electricity, Wiley, New York, London, 1960.
[4] H. Moss, Br. J. Electron. 2 (1957) 305.
[5] G.N. Hatsopoulos, J. Kaye, J. Appl. Phys. 29 (1958) 1124.
[6] J.M. Houston, J. Appl. Phys. 30 (1959) 481.
[7] N.S. Rasor, J. Appl. Phys. 31 (1960) 163.
[8] J.H. Ingold, J. Appl. Phys. 32 (1961) 769.
[9] L.B. Robinson, K. Shimada, J. Appl. Phys. 47 (1976) 107.
[10] G.D. Mahan, J. Appl. Phys. 76 (1994) 4362.
[11] D.M. Rowe, C.M. Bhandari, Modern Thermoelectrics, Holt Technology, Rinehart and Winston, 1983.
[12] G.D. Mahan, J. Appl. Phys. 70 (1991) 8.
[13] D.M. Rowe, G. Min, J. Power Sources 73 (1998) 193.
[14] D.M. Rowe, Renewable Energy 5 (1994) 1470.
[15] D.M. Rowe, Renewable Energy 16 (1999) 1251.
[16] X.C. Xuan, J. Appl. Phys. 92 (2002) 4746.
[17] G.D. Mahan, J. Appl. Phys. 76 (1994) 4362.
[18] C. Wood, Rep. Prog. Phys. 51 (1988) 459.
[19] G.A. Slack, M.A. Hussain, J. Appl. Phys. 70 (1991) 2694.
[20] From http://www.melcor.com, homepage of MELCOR, USA.